JOURNAL OF MATERIALS SCIENCE **39** (2004) 3927–3934

Devitrification of Al-Ni-Rare Earth amorphous alloys

L. BATTEZZATI*, M. KUSY', P. RIZZI, V. RONTO'
Dipartimento di Chimica IFM, Centro di Eccellenza Superfici ed Interfasi Nanostrutturate, Università di Torino, Via Pietro Giuria 9, 10125 Torino, Italy
E-mail: livio.battezzati@unito.it

The effect of rare earth (RE) elements on the devitrification behaviour of $Al_{87}Ni_7RE_6$ alloys (RE = La, Sm) is reported. Two crystallisation mechanisms are found as a function of the type of element and, therefore, size: when RE = La the transformation occurs in two steps, when RE = Sm the transformation has an additional step. The glass transition becomes manifest for both alloys when fast enough rates are used in Differential Scanning Calorimetry. The first crystallisation step implies precipitation of nanocrystalline Al in $Al_{87}Ni_7Sm_6$ and of a metastable intermetallic phase in $Al_{87}Ni_7La_6$, relatively coarse grained. Its formation is suppressed by substitution of 1% at La with Ti or Zr. Interestingly, the amorphous matrix in $Al_{87}Ni_7La_6$ is stabilised by annealing at temperatures below the glass transition so that the second crystallisation peak is shifted to higher temperature. In $Al_{87}Ni_7Sm_6$ the glass transition remains visible after partial crystallisation showing that the matrix is readily homogenised. As a consequence, it transforms abruptly with a polimorphic-like reaction. There is evidence of a calorimetric continuous background for all alloys which is attributed to diffusional homogenisation of the alloy and grain growth. The results are discussed in terms of nucleation and growth mechanisms.

1. Introduction

Al-based amorphous alloys occur in systems containing at least a transition metal (TM) and a rare earth (RE) element. On proper annealing, they tend to form fine Al precipitates in an amorphous matrix. These two-phase alloys have attracted interest because of their improved mechanical properties with respect to both conventional light alloys and amorphous Al alloys [1–4]. Much work has appeared in the recent literature dealing with their devitrification behaviour in view of microstructure optimisation, however, the detailed role of alloying elements is not fully understood. The rare earth elements, as well as Y, are usually considered as vicariant in these alloys although differences in the amorphising range were demonstrated for binary Al-RE and ternary Al-TM-RE systems [5]. A recent systematic study of Al-Ni-Gd alloys has shown that the composition for easier amorphisation is around $Al_{87}Ni_7Gd_6$ [6]. Trends in the crystallisation temperature as a function of Ni or Gd content were reported, but the kinetics of phase transformations was not studied. We started from this finding and substituted various RE elements for Gd. Results for $Al_{87}Ni_7Ce_6$ and $Al_{87}Ni_7Nd_6$ alloys were reported earlier, showing a clear discontinuity in transformation mechanism when using different rare earth elements [7]. With a different approach, the rare earth elements were mixed in several $Al_{88}RE_8Ni_4$ alloys to tailor the average RE radius, and an increasing trend of the glass transition temperature has been shown as a function of the rare earth atomic radius with a sudden drop at larger size. The crystallisation temperature has a less clear dependence on this quantity with fluctuations at low radius and saturation at high radius [8]. The amount of information on devitrification mechanism as a function of the type of element is extended here by analysing $Al_{87}Ni_7RE_6$ systems with RE = La and Sm.

A recent suggestion on transformation mechanism indicates phase separation within the glassy phase as a possible precursor stage to devitrification [9]. To check for evidence of this effect, substitution of part of the rare earth element with Ti and Zr was devised. The rationale behind this choice is that Ti and Zr display positive heat of mixing with rare earth elements but strongly negative with the other alloying elements, so the substitution might force the change in local order within the glassy phase.

2. Experimental

Master alloys were prepared by arc melting suitable quantities of the pure elements in a rare earth gettered atmosphere. Lumps of the master ingots were then rapidly solidified by melt spinning under a protective atmosphere obtained by repeated evacuation and purging

*Author to whom all correspondence should be addressed.

of the apparatus. The sample were contained in a silica crucible which was prepared for the experiment by lining it with a film of rare earth oxide. The coating was obtained by letting a piece of the alloy react with the crucible at high temperature. No further sign of reaction was seen during the use of the crucible. The alloy phases were studied by X-ray diffraction (XRD) with Cu K_α radiation. The microstructure was examined by Transmission Electron Microscopy (TEM) after electrolytic thinning of the samples. A power compensation differential scanning calorimeter (DSC) was used under flowing Argon for scans and anneals up to selected temperatures at various heating rates. The temperature and heat calibrations of the DSC cell were carefully checked at various heating rates with pure metal standards (In, Zn).

3. Results

Figs 1 and 2 show some DSC traces given by $Al_{87}Ni_7La_6$ and $Al_{87}Ni_7Sm_6$ amorphous alloys at various heating rates. The data are the results of the subtraction of a first trace made with the as-quenched alloy and a second trace made with the same alloy after complete transformation to the equilibrium phases. The crystallisation of $Al_{87}Ni_7La_6$ occurs in two steps, that of $Al_{87}Ni_7Sm_6$ in three. Before the occurrence of the first one there is a detectable glass transition at rates as high as 10 and 30 K/min respectively. In both alloys there is a primary transformation occurring with an asymmetric peak. In the temperature ranges between the peaks, the DSC trace hardly returns to the baseline level showing, instead, a slight and continuous output of heat from the sample. The second peak of $Al_{87}Ni_7Sm_6$ shows major changes as a function of heating rate. It occurs progressively at low rates ($\leq$5 K/min), becomes narrow and deep at rates between 10 to 40 K/min and broader at higher rates. The third one is always symmetric and reproduced in its shape. The heat of each transformation and, moreover, the overall heat of crystallisation can be determined only with some scatter. In Figs 1 and 2 it is indicated how a baseline was drawn for the single peaks and for the whole transformation range. With this construction the value of the heat of the individual transformations was reproducible with a scatter amounting roughly to the size of the symbols used in Figs 3 and 4 where the heat of transformation is reported as a function of heating rate. The error involved in the baseline determination is accounted for in the total heat of transformation.

The heat of the first signal increases with heating rate at low rates and then reaches a constant value at high rates for both alloys (Figs 3 and 4). The heat related to the subsequent transformations for both alloys is constant with heating rate. In both alloys, however, the overall heat due to the transformation from the amorphous state to the equilibrium crystalline phases can be considered as constant with heating rate within the experimental uncertainty which is mostly due to the difficulty of constructing a proper baseline, extending below all peaks in a wide temperature interval. In all cases there is a sizeable contribution from a continuous background since the overall heat evolved is definitely higher then the sum of that due to the individual peaks.

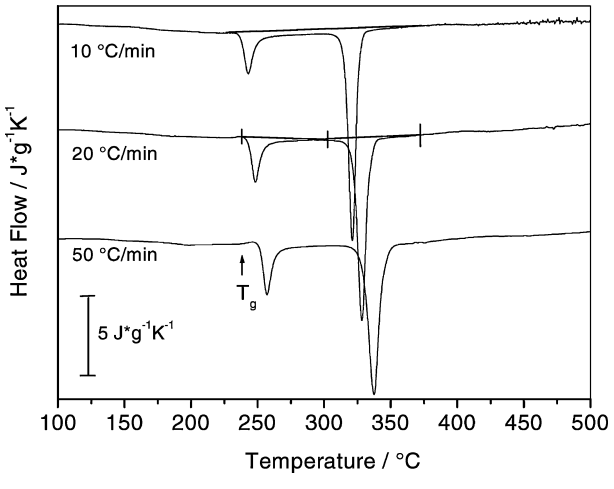

Figure 1 DSC curves for crystallisation of $Al_{87}Ni_7La_6$ at different heating rates. The baseline constructions used to determine the total and partial heat of transformation are shown. The glass transition at one rate is indicated by an arrow.

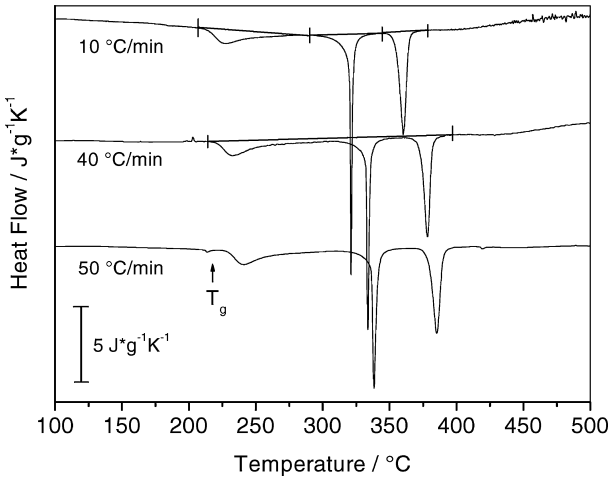

Figure 2 DSC curves for crystallisation of $Al_{87}Ni_7Sm_6$ at different heating rates. The baseline constructions used to determine the total and partial heat of transformation are shown. The glass transition at one rate is indicated by an arrow.

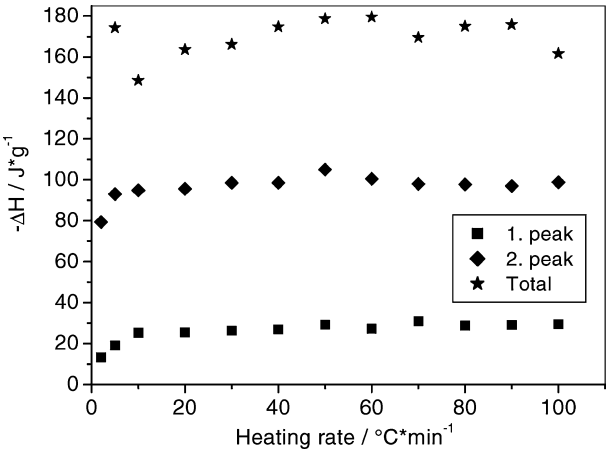

Figure 3 The heat of individual DSC peaks and that for full crystallisation to equilibrium phases as a function of heating rate for the $Al_{87}Ni_7La_6$ alloy.

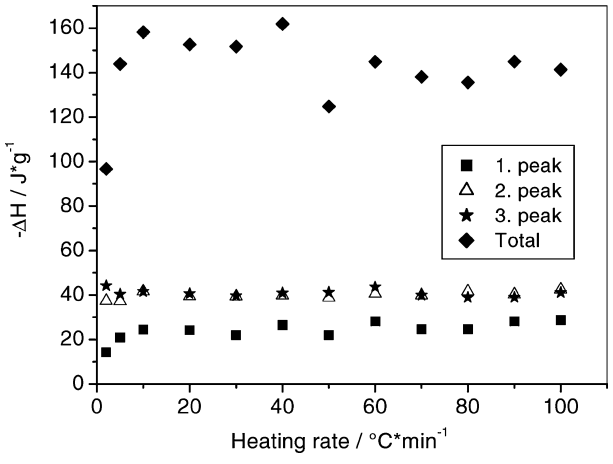

Figure 4 The heat of individual DSC peaks and that for full crystallisation to equilibrium phases as a function of heating rate for the $Al_{87}Ni_7Sm_6$ alloy.

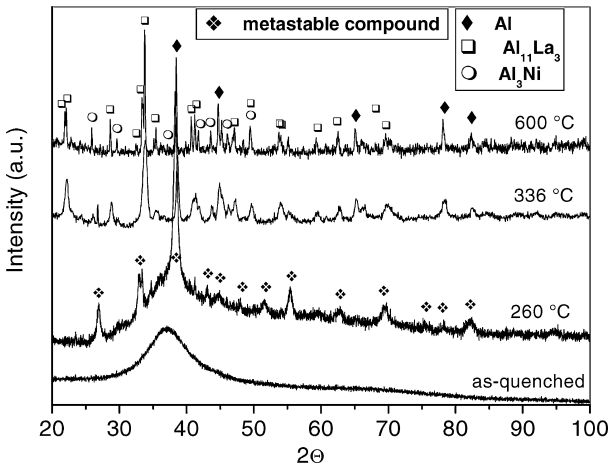

Figure 6 XRD patterns obtained with $Al_{87}Ni_7La_6$ samples annealed up to various temperatures: 260°C is after the first DSC peak, 336°C is right after the second DSC peak.

The variable heat involved in the first transformation and the change in shape of DSC peaks for both alloys, suggest that the transformations are not isokinetic as a function of heating rate. To check this, the ratio of the height of the first to the second peak is plotted in Fig. 5 for both alloys. Should both transformations be isokinetic a constant value would be expected (of course the same would apply to the width at half height). It is apparent that the ratio increases steadily for $Al_{87}Ni_7La_6$ and has a minimum for $Al_{87}Ni_7Sm_6$ showing that the transformation mechanisms depend on heating rate and/or the temperature and time ranges where they occur.

On the other hand, there is no change in the phases which are produced in each DSC peak. Fig. 6 reports XRD patterns for samples heated up to selected temperatures. The first peak for $Al_{87}Ni_7La_6$ is due to precipitation of a metastable intermetallic, possibly rich in the rare earth as suggested by the high intensity of reflections, and the second to transformation of such metastable phase and final crystallisation of the matrix. A detailed analysis of the primary crystallisation and of the structure of the intermetallic compound (primitive cubic, lattice constant: 0.661 nm) is reported elsewhere

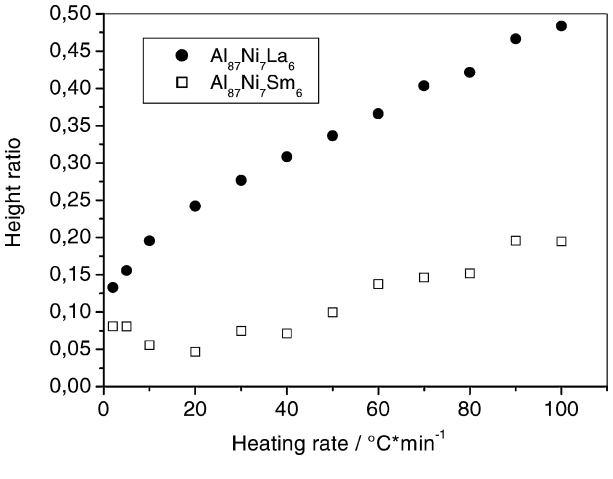

Figure 5 The ratio of the height of the first to the second DSC peak as a function of heating rate for the alloys listed in the insert.

[10]. Here a TEM image and the corresponding SAED pattern are shown in Fig. 7a which demonstrate the occurrence of a phase having the same lattice spacings as those found in XRD patterns. The crystals are rather large and irregular in shape. Note that the mottled contrast of some crystalline areas can be due to the fact that the objective aperture used to take the bright field image did not cover the reflections of the crystal phase closer to the transmitted beam. Therefore, these reflections contributed to the final image. The equilibrium phases are recovered with the second peak: Al, Al_3Ni and $Al_{11}La_3$, as shown in Fig. 6 also with the help of the sharper reflections obtained after annealing up to 600°C. For $Al_{87}Ni_7Sm_6$ during and after the first peak broad reflections of Al appear in addition to the halo corresponding to the remaining amorphous phase (Fig. 8). The TEM image of Fig. 7b shows such fine Al crystals having either dendritic or rounded shape. A few of them must have been corroded preferentially during thinning leaving their ghost image in the photograph. In the XRD pattern of a sample heated up to the end of the second peak (330°C), only Al reflections are identified, more intense than those of the previous pattern, together with broad scattering contributions. Some reflections becomes evident when approaching the third peak (373°C). The structure of the alloy at this stage appears much alike that of $Al_{87}Ni_7Nd_6$ where the broad signals could be assigned to a crystalline intermetallic phase, ruling out the persistence of an amorphous phase at this stage. In the fully crystallised sample and in that heated up to 600°C two phases, Al and $Al_{11}Sm_3$ are easily recognised. The remaining reflections are assigned to Al_7Ni_2Sm in analogy with the phase identified in $Al_{87}Ni_7Nd_6$ which displayed a similar pattern [11]. No differences are found in XRD patterns of samples heated at other rates to the corresponding temperature points.

Isothermal annealings performed to determine the fraction of alloy transformed in the primary reaction, revealed an unexpected feature for $Al_{87}Ni_7La_6$. Fig. 9 reports DSC traces obtained with samples previously annealed for various times at 220°C, i.e., a temperature below the first peak and the glass transition.

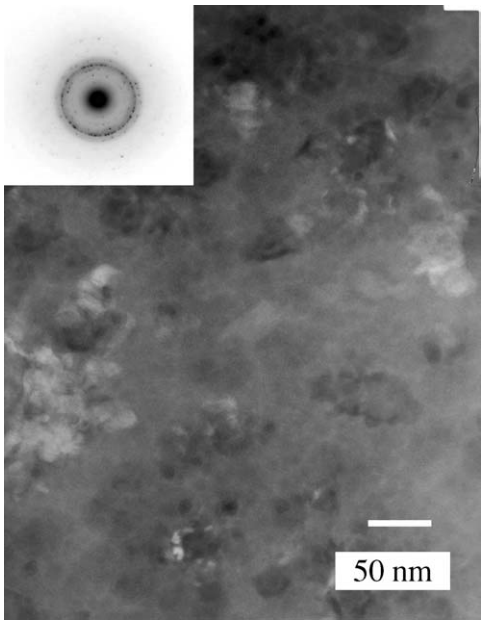

(a)

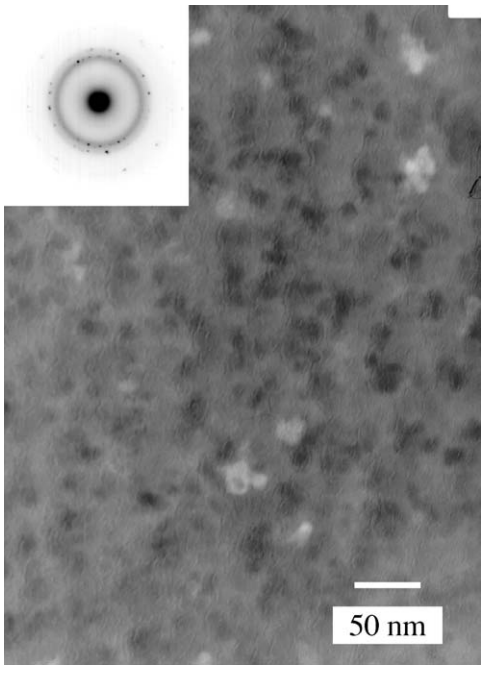

(b)

Figure 7 TEM images and selected area diffraction patterns of samples after primary crystallisation. (a) $Al_{87}Ni_7La_6$ after the first DSC peak, (b) $Al_{87}Ni_7Sm_6$ after the first DSC peak. The patterns can be indexed with the same lattice spacings as for the XRD patterns in Figs 6 and 8.

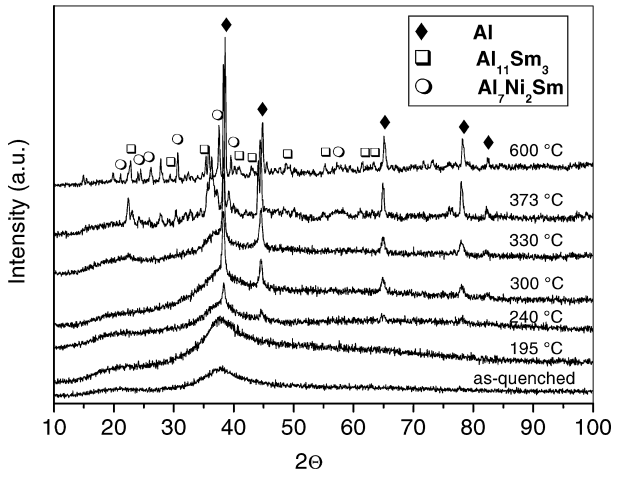

Figure 8 XRD patterns obtained with $Al_{87}Ni_7Sm_6$ samples annealed up to various temperatures: 195°C is before the first DSC peak, 240°C is after the first DSC peak, 300°C is before the second DSC peak, 373°C is right after the second DSC peak.

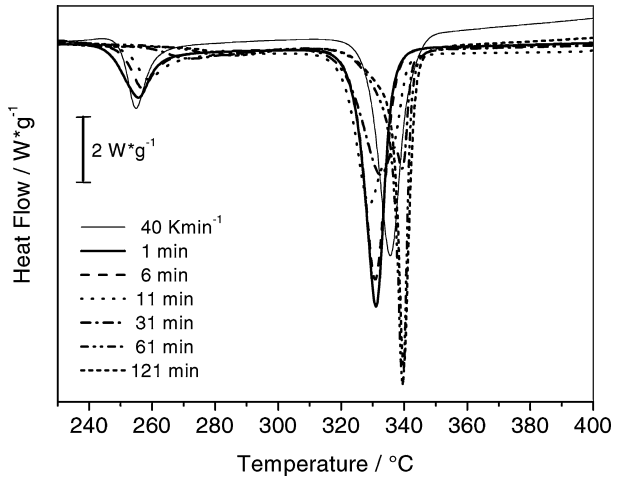

Figure 9 DSC curves for crystallisation of $Al_{87}Ni_7La_6$ obtained after annealing samples at 220°C for the times indicated in the insert. The heating rate is 40°C/min. The thin continuous curve shows the curve obtained in a scan with a sample which was not previously annealed.

Precipitation of the primary phase occurs on annealing so that the relative DSC peak is progressively reduced. Its maximum shifts to higher temperatures the longer the annealing time. This was already found for several alloys based on Al and transition metals. The surprising finding is that the second peak is much affected by the low temperature annealing. For short annealing times the peak is slightly changed in shape but occurs in the same temperature range as for unannealed samples. For longer annealing times a further peak develops some 15 degrees above the previous one which reduces in size and finally disappears. The new peak stands alone after 30 min annealing. Annealings have been performed in the temperature range from 210°C to 230°C obtaining always the same results in different time periods. The intensity of the reflections corresponding to the (200) and (311) angular position in XRD patterns taken on samples annealed at intermediate stages of the transformation, indicated that the formation of the metastable compound takes place together with that of some crystalline Al. The heat released during all transformations is constant (99 $\pm$ 5 J/g) and equals that produced by unannealed samples within the scatter of data.

Analogous isothermal annealings were performed with $Al_{87}Ni_7Sm_6$ samples. The reduction in size and the shift to high temperature of the residual DSC first peak were confirmed, but no major change was found for the second and third peaks.

Amorphous alloys where Ti or Zr substitute for 1% at La were also analysed. In both cases the primary transformation involves precipitation of Al, contrary to the intermetallic phase found in the ternary alloy. Results for $Al_{87}Ni_7La_5Ti$ are given here. The addition of Ti

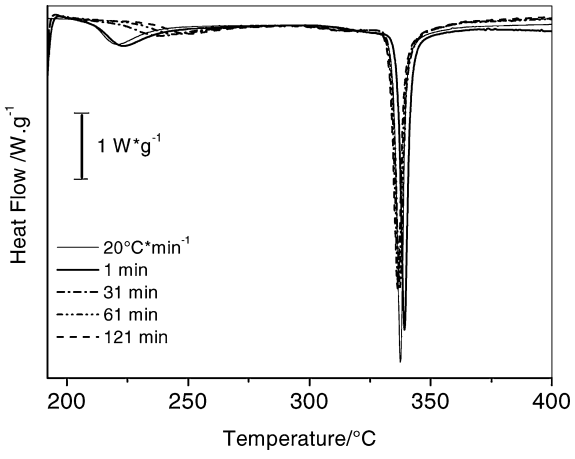

Figure 10 DSC curves for crystallisation of $Al_{87}Ni_7La_5Ti$ obtained after annealing samples at 190°C for the times indicated in the insert. The heating rate is 40°C/min. The thin continuous curve shows the curve obtained in a scan with a sample which was not previously annealed.

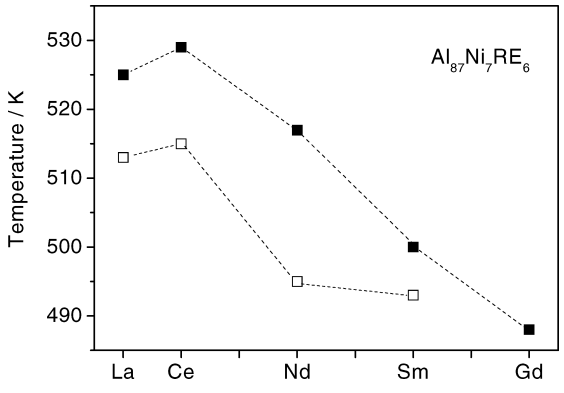

Figure 11 The glass transition temperature (open symbols) and the onset primary crystallisation temperature (full symbols) for $Al_{87}Ni_7RE_6$ amorphous alloys as a function of atomic number. All data refer to 40 K/min heating rate which proved sufficient to get a reliable measure of the inflection of the DSC curve due to T_g by means of geometrical construction with the exception of the point for Sm which had to be obtained at the heating rate of 150 K/min.

lowers the primary crystallisation temperature but the overall shape of the DSC trace is not changed apart from a tiny shoulder which appears just before the second peak. Fig. 10 reports DSC traces obtained with samples previously annealed for various times at 190°C. The first peak is reduced in size and shifted to high temperature. The second one remains to all effects unchanged. The only further effect of low temperature annealing is the shift to low temperature of the shoulder of the second peak. It actually turns to a small peak after annealing. Careful XRD analyses of samples annealed at 190°C for 120 min and heated up to 315°C at 20°C/min show that the small peak is due to formation of $Al_{11}La_3$ mostly on the air side of the ribbon.

4. Discussion

In $Al_{87}Ni_7La_6$ and $Al_{87}Ni_7Sm_6$ the inflection of the DSC trace due to T_g starts being detected at rates higher than 10°C/min and 30°C/min, respectively, otherwise it is fully overlapped by the first crystallisation event [11]. When samples are annealed below the first peak to induce partial precipitation, the composition of the matrix changes, so does its glass transition temperature. In order to detect the new T_g the crystallisation of the primary phase should be over and growth limited so that no exothermal effect will shadow the endothermal signal due to the glass transition. Furthermore, the glassy phase must be largely homogeneous in composition in order to present the transition in a definite temperature range. All these requirements are rarely met in partially crystallised metallic glasses. An example was reported for amorphous $Al_{87}Ni_7Nd_6$ annealed 120 min at 200°C [7]. The DSC trace obtained on continuous heating the annealed samples had a clear T_g. This results has been reproduced in this work when annealing the $Al_{87}Ni_7Sm_6$ for more than 90 minutes at 190°C. On the other hand, the $Al_{87}Ni_7La_6$ alloy does not reach the level of homogeneity needed for T_g to be detected.

When Sm substitutes for La in the alloy there is a major change in transformation mechanism from two to three stages. Ternary alloys with Sm behave as those containing Y [12], Gd [6] and Nd but the alloy with La is alike $Al_{87}Ni_7Ce_6$. This is correlated to the formation of an unknown intermetallic in the case of RE = Nd and Sm and, possibly to the size of the elements, the smaller ones (Nd, Sm, Gd, Y) causing transformation in three stages and the larger ones (La, Ce) in only two. Moreover the final products of crystallisation are Al, $Al_{11}RE_3$ and Al_3Ni for RE = La and Ce whereas they are Al, $Al_{11}RE_3$ and Al_7Ni_2RE for RE = Nd and Sm. It is concluded that there is a major effect of the rare earth element on crystallisation mechanism. The onset crystallisation temperature and the glass transition temperature for $Al_{87}Ni_7RE_6$ alloys are collected in Fig. 11. Both temperatures and their difference, a quantity linked to glass formability, decrease on decreasing element radius from La to Gd. This plot confirm the recent report that the ease of glass formation and the glass transition temperature depend on the size of the rare earth atoms used for alloying and both properties worsen with either smaller and larger rare earths and show a maximum at intermediate sizes [8].

The change in shape of the DSC peaks shows that the transformations are not isokinetic. The shape of the second peak of $Al_{87}Ni_7Sm_6$ displays a major change as a function of heating rate confirming data already obtained with $Al_{87}Ni_7Nd_6$ [7]. It is skewed on the low temperature side at low rates, then becomes very narrow at intermediate rates and finally broadens steadily at high rates. Note, however, that the peak starts progressively in all cases. After this slow start it has an abrupt emission of heat beginning at the heating rate of 10 K/min. Actually, the half width of all peaks obtained at 10 K/min and higher heating rates corresponds to the same amount of time. This means that the transformation becomes independent of heating rate as soon as it is started i.e. it becomes autocatalytic. The peaks are still displaced on the temperature axis according to heating rate, but this is due to the thermal activation of the early stages before they develop abruptly.

The number density of Al crystals in partially crystallised $Al_{87}Ni_7Sm_6$ is large as judged from Fig. 7b where crystals are seen ranging from 10 to 30 nm in size,

distant from each other less than 50 nm. This is the result of copious nucleation of homogeneously distributed particles. There has been discussion on the nature of the nucleation events. When analysing the crystallisation of binary Al-Sm alloys it was suggested that, being the crystals so copious, nucleation might have been mostly homogeneous. This was compatible with the shape of the size distribution of nanocrystals [13, 14]. Moreover, impurities and inclusions found in the material would not have accounted for all crystals formed if they acted as heterogeneous nucleants. Subsequent experiments on glassy $Al_{82}Sm_8$ alloys either melt quenched and obtained by cold rolling foils of the elements showed a clear difference in crystallisation mode between the two materials: the melt quenched samples contained the expected high population of nanocrystals after annealing through the primary crystallisation whereas this was fully avoided in the cold rolled material. The conclusion was then drawn that the nanocrystals should have been produced by growth on pre-existing seed which could have been formed during quenching whereas the seeds were not present in the solid state processed alloy [15]. However, later an analysis of the size distribution of the nanocrystals led to conclude that after an initial nucleation on quenched-in clusters thermal nucleation could have followed to complete the reaction [16]. So, it is likely that a single nucleation mechanism does not apply. The varied shapes, either branched or rounded, of the Al nanocrystals found in $Al_{87}Ni_7Sm_6$ should be judged in view of these considerations.

Since the Al-RE compounds melt at high temperature, it is expected that the driving force for their nucleation is high in the temperature range of the DSC peaks. It was shown that the driving force levels off at high undercooling because of the progressive stabilisation of the liquid phase due to the excess liquid specific heat, although remaining higher than that for Al [17]. The two type of phases compete for nucleation and factors such as glass (liquid)-crystal interfacial tension can become decisive in phase selection. It is expected that the simple fcc structure of low-melting Al will involve a lower interfacial tension with respect to the complex $Al_{11}Nd_3$ compound having high melting point. In addition, pre-existing seeds would lower the interfacial tension acting as nucleants [18]. On the other hand, metastable compounds may display short range order closer to that of the glass (liquid) and, therefore, nucleate preferentially.

In partially crystallised $Al_{87}Ni_7La_6$ the crystals of the intermetallic phase are definitely larger and less frequent (Fig. 7a). Their size is variable but always exceeds 50 nm. At this stage no definitive hypothesis can be made on their origin even if the presence of large crystals after heating up to the first peak, is indicative of formation by growth of nuclei built up during quenching. This would explain the saturation in crystallisation temperature seen for the La and Ce containing $Al_{87}Ni_7RE_6$ alloys in Fig. 11 which reproduces that reported in [8] for a series of other alloys where the same phase forms. In fact, it is expected that growth induced by mobility of rare earth elements of similar size would be activated much in the same way in the Al-Ni matrix.

During primary devitrification of Al in a $Al_{87}Ni_{10}Ce_3$ alloy, it was found that rare earth atoms accumulate ahead of the nanocrystal interface whereas Ni diffuses faster in the matrix [19], so its concentration is more readily homogenised. On the other hand, no increase in Sm concentration at the Al-matrix interface could be detected in an $Al_{88}Ni_4Sm_8$ alloy [20]. The present findings point to the existence of asymmetric DSC peaks for the first transformation and a continuous background in the DSC signal for both $Al_{87}Ni_7La_6$ and $Al_{87}Ni_7Sm_6$. These are related to the combined effect of diffusional mixing in the matrix, implying interfacial solute build up, and growth of the primary phase. However, once all contributions due to crystallisation are summed up, the enthalpy due to the background is more limited for $Al_{87}Ni_7Sm_6$ (about 20 J/g) with respect to $Al_{87}Ni_7La_6$. So, it can be concluded that the diffusional gradient must be more limited in the former case. The second transformation of the latter alloy which involves decomposition of a metastable intermetallic and crystallisation of the matrix always occurs when the matrix is not yet homogenised on continuous heating, contrary to the latter alloy where the abrupt occurrence of the second peak indicates fast transformation, possibly polymorphic, of a homogeneous matrix. Since both transformations occur in the same temperature range, it is inferred that the extent of diffusion fields which is suggested as a key factor in restraining nucleation and stabilising the two-phase microstructure, is less relevant in these materials with respect to the sluggish diffusivity of solute elements.

A remarkable feature which must be linked to the above discussion on matrix homogenisation, is the shift of the second peak of $Al_{87}Ni_7La_6$ to high temperature after annealing for some time at temperatures below the first peak as shown in Fig. 9. There is no sign of such effect in DSC scans performed at rates as low as 1 K/min. The two peaks shift regularly as a function of heating rate and can be used for constructing Kissinger plots. Deviation from the linearity of such plots is found only when using rates high enough to displace the first peak entirely in the undercooling regime, i.e., above the glass transition temperature [11]. XRD analyses show that after the first peak on continuous heating the primary phase is a metastable intermetallic. On the other hand, after isothermal annealing patterns are compatible with the formation of Al together with the same intermetallic. Since the reflections of the two phases fully overlap, this is suggested by the higher intensity of reflections falling in the angular range of those of Al, e.g., (200), (311). With this hypothesis, the shift to high temperature of the second peak, i.e., the stabilisation of the matrix, would occur when enough Al has precipitated together with the metastable compound.

From the high intensity of relevant XRD reflections it is inferred that the metastable compound found at the intermediate stage in $Al_{87}Ni_7La_6$ is rich in La. Actually, this phase is not found in alloys containing lower amount of La. In the present work it is shown with the $Al_{87}Ni_7La_5Ti$ alloy that the primary crystallisation mode changes when reducing the La content of 1% in atoms. Since a metastable compound is formed also in

the analogous alloy containing 6% at Ce, but not in that containing 3% at Ce, it is concluded that the formation of such compounds occurs when the rare earth content reaches about 6% at.

Considering now the composition of the amorphous matrix remaining after primary crystallisation, it is clearly enriched in all solutes when Al precipitation occurs. This, however, does not determine the subsequent transformation sequence since three stages are found for $Al_{87}Ni_7Sm_6$ and two for $Al_{87}Ni_7La_5Ti$. In the case of $Al_{87}Ni_7La_6$ the precipitation of a La rich compound will leave a matrix enriched in Ni. This is again rather unexpected since binary Al-Ni alloys cannot be vitrified by rapid solidification and at least 2–3% in atoms of the glass-former rare earth atoms are needed for amorphisation [1]. Actually, the Al-RE compounds tend to crystallise earlier than Al_3Ni. It was found, in fact, by careful inspection of XRD patterns, that the prepeak appearing before the second crystallisation stage in $Al_{87}Ni_7La_5Ti$ is due to the formation of a small quantity of $Al_{11}La_3$. The stability of amorphous phases rich in Ni correlates well with the more negative heat of mixing in the liquid state of Al-Ni with respect to Al-La [for collection of data see Refs. 21 and 22, respectively].

The use of 1% Ti instead of La was meant to enhance phase separation within the amorphous phase which has been claimed in some Al-Ni-RE alloys. Specifically, the demixing of the amorphous phase has been reported after annealing for 1 min at 223°C a $Al_{87}Ni_4La_2Gd_6$ amorphous alloy [23]. The short term annealings performed on $Al_{87}Ni_7La_6$ and $Al_{87}Ni_7La_5Ti$ should be suited to check for this effect. After 1 min annealing at 220 and 230°C XRD patterns of $Al_{87}Ni_7La_6$ samples already showed sign of crystallisation of the metastable compound discussed above. The existence of a crystalline fraction accounts for the broadening of the DSC peak found with the annealed sample with respect to an as-quenched one. For the annealed $Al_{87}Ni_7La_5Ti$ both the XRD patterns and DSC scans did not show significant changes. Therefore, a thermal and structural effect of amorphous phase demixing has not been found up to now in these alloys.

5. Conclusions

By analysing $Al_{87}Ni_7La_6$ and $Al_{87}Ni_7Sm_6$ amorphous alloys, in this paper support has been given to the finding that the devitrification mechanism strongly depends on the type and size of RE element as suggested in previous work on Al-Ni-RE amorphous alloys containing Ce and Nd. This is shown by the different number of transformations occurring in the two alloys, two and three respectively, and by the trend of the glass transition and crystallisation temperatures as a function of atomic number.

The primary transformation involves precipitation of Al nanocrystals in $Al_{87}Ni_7Sm_6$ and of a La rich metastable phase in $Al_{87}Ni_7La_6$. It has been shown by substituting 1% at of La with Ti that the formation of the metastable intermediate can be suppressed obtaining the precipitation of Al. The formation of such a compound does not occur at rare earth content lower than 6% at. Therefore, caution should be taken in designing the alloy composition if precipitation of Al is desired for improved mechanical properties.

From the reduced number and larger size of crystals it is inferred that the nucleation of the primary metastable phase in $Al_{87}Ni_7La_6$ has possibly occurred via a heterogeneous mechanism on quenched-in nuclei. The formation of high number of Al crystals of small size in $Al_{87}Ni_7Sm_6$ can probably be interpreted with a mixed mechanism of nucleation on pre-existing clusters and thermally assisted nucleation of new particles.

Analyses of heat evolution in DSC have shown that the diffusional homogenisation of the amorphous matrix contributes significantly to the overall DSC signal over a wider temperature range for $Al_{87}Ni_7La_6$ than for $Al_{87}Ni_7Sm_6$. Therefore, crystallisation of the remaining amorphous matrix occurs in the presence of compositional gradients only in the former alloy although the temperature range of transformation is similar. Such gradients are usually considered as necessary for stabilisation of the two phase microstructure. Here it is suggested that also the low mobility of the solute elements is relevant for the same purpose.

An unexpected finding is that the amorphous matrix can be stabilised, i.e., the second crystallisation stage displaced some twenty degrees in temperature, by isothermal annealing the alloy at temperatures below the first transformation peak. With the evidence available at present, this correlates with the formation of Al crystals together with those of the metastable compound on isothermal annealing. The outcome is the coexistence of three phase in metastable equilibrium, more stable than the phase mixture of the intermetallic compound embedded in the inhomogeneous amorphous matrix obtained during primary crystallisation.

Acknowledgement

This work is partly funded by the Research Training Network of the European Commission "Nano Al" HPRN-CT-2000-00038.

References

1. A. INOUE, *Progress Mater. Sci.* **43** (1998) 365.
2. A. INOUE and H. KIMURA, *J. Light Met.* **1** (2001) 31.
3. L. BATTEZZATI, S. POZZOVIVO and P. RIZZI, in "Nanocrystalline Aluminium Alloys," Nanoclusters and Nanocrystals, edited by H. S. Nalwa (American Scientific Pub., Stevenson Ranch, CA, February 2003).
4. G. WILDE, N. BOUCHARAT, R. J. HEBERT, H. RÖSNER, W. S. TONG and J. H. PEREPEZKO, *Adv. Eng. Mater.* **5** (2003) 125.
5. A. INOUE, K. OHTERA and T. MASUMOTO, *Sci. Rep. RITU* A **35** (1990).
6. F. Q. GUO, S. J. POON and G. J. SHIFLET, *Mater. Sci. Forum* **331–337** (2000) 31.
7. L. BATTEZZATI, S. POZZOVIVO and P. RIZZI, *Mater. Trans.* **43** (2002) 2593.
8. A. K. GANGOPADHYAY and K. F. KELTON, *Phil. Mag.* A **80** (2000) 119.
9. A. K. GANGOPADHYAY, T. K. CROAT and K. F. KELTON, *Acta Mater.* **48** (2000) 4035.
10. V. RONTO', L. BATTEZZATI, A. R. YAVARI, M. TONEGARU, N. LUPU and G. HEUNEN, *Scripta Mater.* **50** (2004) 839.

11. L. BATTEZZATI, P. RIZZI and V. RONTO', *Mater. Sci. Eng.* A, in print.
12. R. SABET-SHARGHI, Z. ALTOUNIAN and W. B. MUIR, *J. Appl. Phys.* **75** (1994) 4438.
13. P. RIZZI, C. ANTONIONE, M. BARICCO, L. BATTEZZATI, L. ARMELAO, E. TONDELLO, M. FABRIZIO and S. DAOLIO, *Nanostruct. Mater.* **10** (1998) 767.
14. L. BATTEZZATI, *Mater. Res. Soc. Symp. Proc.* **400** (1996) 191.
15. G. WILDE, H. SIEBER and J. H. PEREPEZKO, *Scripta Mater.* **40** (1999) 779.
16. J. H. PEREPEZKO, R. J. HEBERT, R. I. WU and G. WILDE, *J. Non-Crystalline Solids* **317** (2003) 52.
17. M. BARICCO, F. GAERTNER, P. RIZZI, L. BATTEZZATI, G. CACCIAMANI and A. L. GREER, *Mater. Sci. Forum* **269–272** (1998) 553.
18. J. H. PEREPEZKO, R. J. HEBERT and W. S. TONG, *Intermetallics* **10** (2002) 1079.
19. K. HONO, Y. ZHANG, A. P. TSAI, A. INOUE and T. SAKURAI, *Scripta Metall. et Mater.* **32** (1995) 191.
20. T. GLORIANT, D. H. PING, K. HONO, A. L. GREER and M. D. BARO', *Mater. Sci. Eng.* A, **304–306** (2001) 315.
21. I. ANSARA, N. DUPIN, H. L. LUKAS and B. SUNDMAN, *J. Alloys Comp.* **247** (1997) 20.
22. G. CACCIAMANI and R. FERRO, *Calphad* **25** (2001) 583.
23. K. F. KELTON, T. K. CROAT, A. K. GANGOPADHYAY, L.-Q. XING, A. L. GREER, M. WEYLAND, X. LI and K. RAJAN, *J. Non-Crystalline Solids* **317** (2003) 71.